Volume 22
Number 35
21 September 2024
Pages 7063-7246

# Organic & Biomolecular Chemistry

rsc.li/obc

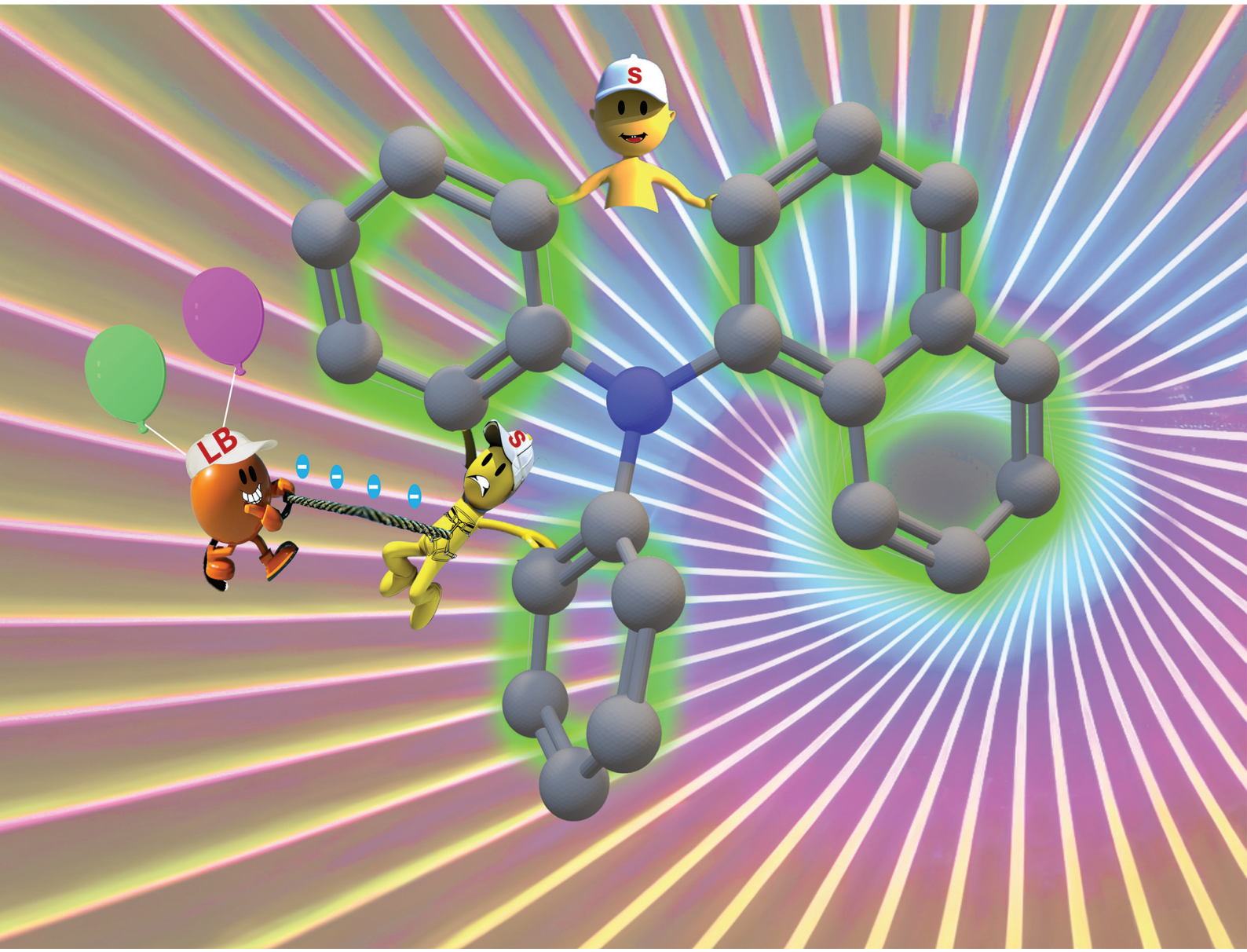


ISSN 1477-0520

ROYAL SOCIETY OF CHEMISTRY

**PAPER**

Michela Lupi, Stefano Menichetti *et al.*
Organocatalytic hydrogen bond donor/Lewis base (HBD/LB) synthesis and chiroptical properties of thiabridged [5] helicenes

Organic & Biomolecular Chemistry

ROYAL SOCIETY OF CHEMISTRY

PAPER

View Article Online
View Journal | View Issue



Check for updates

Cite this: *Org. Biomol. Chem.*, 2024, **22**, 7154

# Organocatalytic hydrogen bond donor/Lewis base (HBD/LB) synthesis and chiroptical properties of thiabridged [5]helicenes†

Michela Lupi, *[a] Mosè Fabbri,[a] Giuseppe Mazzeo,[b] Giovanna Longhi,[b] Sergio Abbate,[b] Caterina Viglianisi[a] and Stefano Menichetti *[a]

Received 11th June 2024,
Accepted 9th July 2024

DOI: 10.1039/d4ob00979g

rsc.li/obc

Thiabridged [5]helicenes are obtained from thioaryl-*N*-phthalimido benzo[*a*]phenothiazines using a hydrogen bond donor/Lewis base organocatalytic approach. Resolution of [5]helicenes using either (1*S*)-(−)-camphanic acid as a chiral auxiliary or CSP-HPLC is reported. Thiabridged [5]helicenes show an exceptional configurational stability with racemization energy barriers higher than 40 kcal mol$^{-1}$. Electronic circular dichroism and TD-DFT calculations permit the assignment of the absolute configuration, demonstrating that the sign of optical rotation is not easily related to the *M* or *P* structure. Separated enantiomers show circularly polarized luminescence with high dissymmetry ratio.

## Introduction

In the last few years, helicenes have played a pivotal role in many fields, such as asymmetric synthesis,[1–3] medicinal chemistry,[4–6] molecular recognition[7,8] and, first and foremost, material science.[9–12] Indeed, several (asymmetric) syntheses of helicenes using transition metal catalysts[13–18] or organocatalysts[19–22] have been reported. Thiabridged [4]helicenes appear particularly attractive, due to their peculiar structure and their ability to be reversibly oxidized to the corresponding radical cations.[23,24] The configurational stability, with racemization energy barriers of ≃32 kcal mol$^{-1}$, allows the enantiopure forms to be handled after HPLC resolution on a chiral stationary phase.[25] Thus, we previously studied the deposition of enantiopure [4]helicene radical cations on a Au(111) surface, proving that both the handedness and paramagnetism are retained after the deposition process.[26] Additionally, after a chemisorbed deposition process, we demonstrated for these molecules an extremely high spin filtering capability at very low voltages.[27] Additionally, the use of these systems as recyclable organophotoredox catalysts has been reported, further extending the fields of application of these thiahelicenes.[28] We recently developed a new organocatalytic strategy for the synthesis of these thiahelicenes from arylthio-*N*-phthalimido precursors using a Lewis base/hydrogen bond donor (LB/HBD) catalytic system.[29] In particular, a selection of simple selenium and sulfur-containing Lewis bases were successfully used in catalytic amounts (10% mol loading) in the presence of hexafluoro isopropanol (HFIP) as a hydrogen bond donor. This methodology allowed thiahelicenes to be obtained in good yields under very mild reaction conditions, avoiding the use, as cyclization promoters, of over-stoichiometric amounts of strong Lewis acids.

The need to obtain helicenes in enantiopure form and in substantial amounts is indeed more and more urgent, possibly avoiding the drawbacks connected with HPLC resolutions.[25] The preparation of enantiopure helicenes on a multi-mg scale

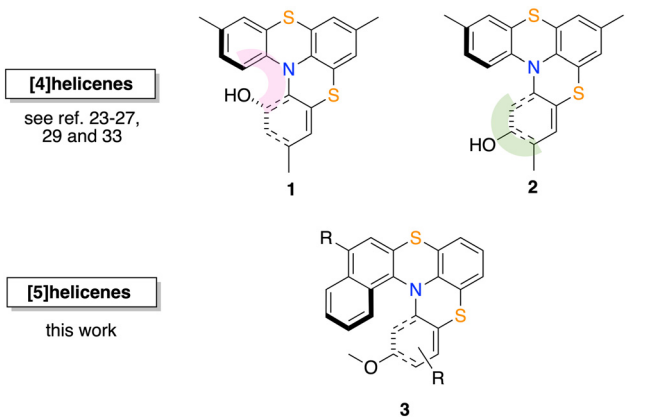


**Fig. 1** Structure of thiabridged [4]helicenes and [5]helicenes.

[a]*Department of Chemistry "Ugo Schiff" (DICUS), University of Florence, Via della Lastruccia 13, Sesto Fiorentino (FI), 50019 Florence, Italy. E-mail: michela.lupi@unifi.it, stefano.menichetti@unifi.it*
[b]*Department of Molecular and Translational Medicine (DMMT), University of Brescia, V. le Europa 11, Brescia (BS), 25121 Brescia, Italy*

†Electronic supplementary information (ESI) available. CCDC 2361198–2361200. For ESI and crystallographic data in CIF or other electronic format see DOI: https://doi.org/10.1039/d4ob00979g

was previously accomplished mainly for [5]-[30] or [6]helicenes[31] using an optical resolution approach. Nevertheless, just a few examples of optical resolution of [4]helicene derivatives are reported in the literature, due to the lower configurational stability.[32]

Recently, we demonstrated that chemical resolution can be achieved also for configurationally stable and properly substituted (*vide infra*) hydroxy thiabridged triarylamine [4]helicenes forming mixtures of diastereoisomeric esters, separable by flash column chromatography, exploiting properly selected enantiopure carboxylic acids.[33] The success of the resolution depends upon a combination of the structure of the enantiopure acid used, with (1*S*)-(−)-camphanic acid giving the best results, and the position of the chiral auxiliary insertion. In fact, separation was effective only for the diastereomers obtained from helicene **1**, bearing the hydroxyl group in the helicene *bay*-zone (*in pink*, Fig. 1, top left). Indeed, the resolution completely failed when the chiral auxiliary was inserted in the helicene **2**, bearing the hydroxyl group in the *cape*-zone (in green, Fig. 1, top right), regardless of the structure of the chiral auxiliary used. Herein, we report the synthesis of hetero [5]helicenes **3** from arylthio-*N*-phthalimido benzo[*a*]phenothiazines **4** using Lewis base/HBD methodology, and a demonstration of how the aromatic backbone expansion improves the chiroptical properties,[34] simplifies chemical resolutions, and increases configurational stability compared to the corresponding [4]helicenes.

## Results and discussion

### Synthesis

**Synthesis of arylthio-*N*-phthalimido benzo[*a*]phenothiazines 4.** The synthetic route to arylthio-*N*-phthalimido benzo[*a*]phenothiazines **4a–d** (*i.e.* precursors of [5]helicenes) is highlighted in Scheme 1.

Benzo[*a*]phenothiazines **7** can be obtained following the metal-free procedure reported by Lin *et al.*[35] by reacting 2-aminothiophenol **5** with tetralones[36] **6a** and **6b** in DMSO under an air atmosphere. Derivatives **7a** and **7b** undergo *N*-arylation by Buchwald Hartwig reaction with electron-rich aryl bromides **8a** and **8b** allowing access to *N*-aryl benzo[*a*]phenothiazines **9a–d** in medium to good yields. Subsequent reaction of **9a–d** with phthalimidesulfenyl chloride delivered sulfenylated products **4a**, **4c** and **4d** with complete regioselectivity. It is worth mentioning that for trimethoxy-substituted derivative **4b**, the naphthalene portion is particularly activated towards $S_EAr$, causing an over-substitution process. Indeed, the reaction led to both the mono-sulfenylated product **4b1** and the bis-sulfenylated product **4b2** (Scheme 1). In fact, reacting **9d** ($R^1 = CH_3$) with PhtNSCl afforded exclusively mono sulfenylated derivative **4d** in 90% yield.

**Synthesis of [5]helicenes.** Sulfenylated phenothiazine **4a** was chosen as a model substrate for the cyclization study, and the formation of helicene **3a** was evaluated by measuring the conversion by $^1$H NMR.

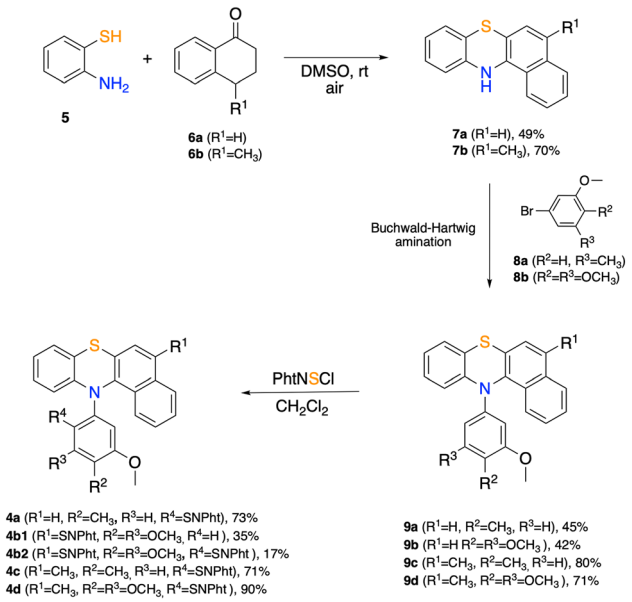


**5**

**6a** ($R^1$=H)
**6b** ($R^1$=$CH_3$)

**7a** ($R^1$=H), 49%
**7b** ($R^1$=$CH_3$), 70%

**8a** ($R^2$=H, $R^3$=$CH_3$)
**8b** ($R^2$=$R^3$=$OCH_3$)

**4a** ($R^1$=H, $R^2$=$CH_3$, $R^3$=H, $R^4$=SNPht), 73%
**4b1** ($R^1$=SNPht, $R^2$=$R^3$=$OCH_3$, $R^4$=H ), 35%
**4b2** ($R^1$=SNPht, $R^2$=$R^3$=$OCH_3$, $R^4$=SNPht ), 17%
**4c** ($R^1$=$CH_3$, $R^2$=$CH_3$, $R^3$=H, $R^4$=SNPht), 71%
**4d** ($R^1$=$CH_3$, $R^2$=$R^3$=$OCH_3$, $R^4$=SNPht ), 90%

**9a** ($R^1$=H, $R^2$=$CH_3$, $R^3$=H), 45%
**9b** ($R^1$=H $R^2$=$R^3$=$OCH_3$ ), 42%
**9c** ($R^1$=$CH_3$, $R^2$=$CH_3$, $R^3$=H), 80%
**9d** ($R^1$=$CH_3$, $R^2$=$R^3$=$OCH_3$ ), 71%

**Scheme 1** Synthetic route to *arylthio-N*-thiophthalimido benzo[*a*]phenothiazines **4**.

In contrast to the synthesis of thia[4]helicenes,[23–27] the use of stoichiometric amounts of $AlCl_3$ in $CH_2Cl_2$ or $CHCl_3$ caused a severe decomposition of starting material **4a** with very low conversion values either at 60 °C or at room temperature (Table 1, entries 1 and 2). Hence, we moved to a new synthetic procedure that exploits hexafluoro isopropanol (HFIP) as a

**Table 1** Cyclization optimization of **4a** to **3a**

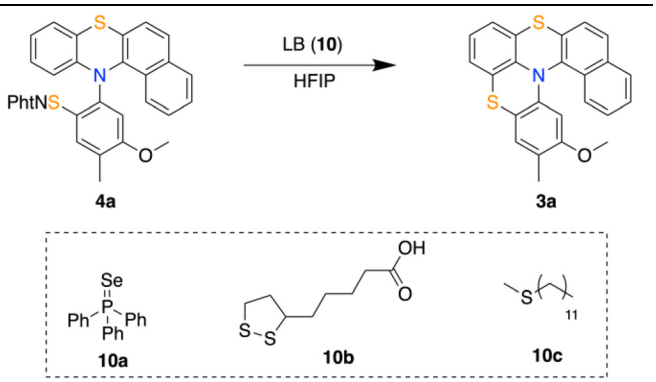


**4a** **3a**

**10a** **10b** **10c**

| Entry | Cat. | Eq. | Solv. | *T* (°C) | Time | Conv.[a] | Yield[b] |
|---|---|---|---|---|---|---|---|
| 1 | $AlCl_3$ | 1.5 | $CH_2Cl_2$[c] | 20 | 2 | — | — |
| 2 | $AlCl_3$ | 1.5 | $CHCl_3$[c] | 60 | 2 | 11 | — |
| 3 | **10a** | 0.10 | HFIP[d] | 20 | 48 | 5 | — |
| 4 | **10a** | 0.10 | HFIP[d] | 50 | 48 | 6 | — |
| 5 | **10b** | 0.10 | HFIP[d] | 20 | 24 | 17 | — |
| 6 | **10b** | 0.40[e] | HFIP[d] | 50 | 24 | 80 | 55 |
| 7 | **10c** | 0.10 | HFIP[d] | 20 | 48 | 50 | — |
| 8 | **10c** | 0.10 | HFIP[d] | 50 | 48 | 70 | 56 |

[a] Measured by $^1$H NMR. [b] Isolated yields after flash column chromatography carried out for conversions > 50%. [c] 0.1 M. [d] 40 mg of **4a** in 200 μL of HFIP. [e] Added in four aliquots every 4 hours.

strong HBD and a catalytic amount of a chalcogen LB.[29] Therefore, a selection of Lewis bases that delivered the [4]helicenes in the highest conversions were evaluated in the presence of HFIP (see Table 1, entries 3–8). Formation of helicene **3a** was initially monitored by $^{1}$H NMR, and, for satisfactory conversion values (higher than 60%), the crude mixture was purified by flash chromatography and the isolated yield of **3a** was evaluated. Racemic lipoic acid (**10b**) and dodecyl methyl sulfide (**10c**) gave the best results in terms of conversion and isolated yields (Table 1, entries 5–8). However, 40% mol of lipoic acid (**10b**) added in four aliquots every 4 h was necessary to parallel the yield of **3a** achieved using 10% mol of dodecyl methyl sulfide (**10c**) (entry 6 *vs.* entry 8).

Thus, the conditions reported in entry 8 of Table 1 were chosen for the substrate scope study. When arylthio-*N*-phthalimido benzo[*a*]phenothiazines **4c** and **4d** were reacted under the optimized conditions, each of the desired [5]helicenes **3c** and **3d**, isolated respectively in 22% and 42% yield, were accompanied by a not negligible amount of a second product (Scheme 2). These unknown products were successfully isolated by flash chromatography. $^{1}$H NMR and $^{13}$C NMR analyses did not elucidate the structure of these by-products, but suggested a helical skeleton similar to that of **3c** and **3d** (see Experimental section and ESI†). Thus, we envisioned the formation of the pleiadene-like molecules **11c** and **11d** (see Scheme 2) as a result of a $S_EAr$ reaction involving the electron-rich *peri* position on the naphthalene ring. Eventually, together with those of helicenes **3a** and **3d**, suitable crystals for X-Ray analysis of the unknown products were obtained (Scheme 2). Thus, the structure of **3a** and **3d** was confirmed and the skeleton of the unknown derivative was disclosed as that of [5]helicene **12d**. With this structure in hand, we assumed that the cyclization of **4c** would afford, along with **3c**, also [5]helicene **12c**. A mechanism suitable to rationalize the formation of the expected helicene **3d** (and **3c**) together with the unexpected helicene **12d** (and **12c**) is highlighted in Scheme 3. Path A (pink frame): arylthio-*N*-phthalimido derivative **4d** reacts with dodecyl methyl sulfide (**10c**) to form charged intermediate **i1**, which undergoes an intramolecular $S_EAr$ ($iS_EAr$) to form the Wheland intermediate **i2** that can evolve into helicene **3d**. Path B (green frame): intermediate **i2** undergoes a rearrangement to give the Wheland intermediate **i3**, which in the presence of catalyst **10c** forms intermediate **i4** (*i.e.* a retro-$iS_EAr$), and eventually affords [5]helicene **12d** *via* intermediate **i5**. As a matter of fact, when helicenes **3d** or **12d** were placed under the HBD/LB reaction conditions, no for-

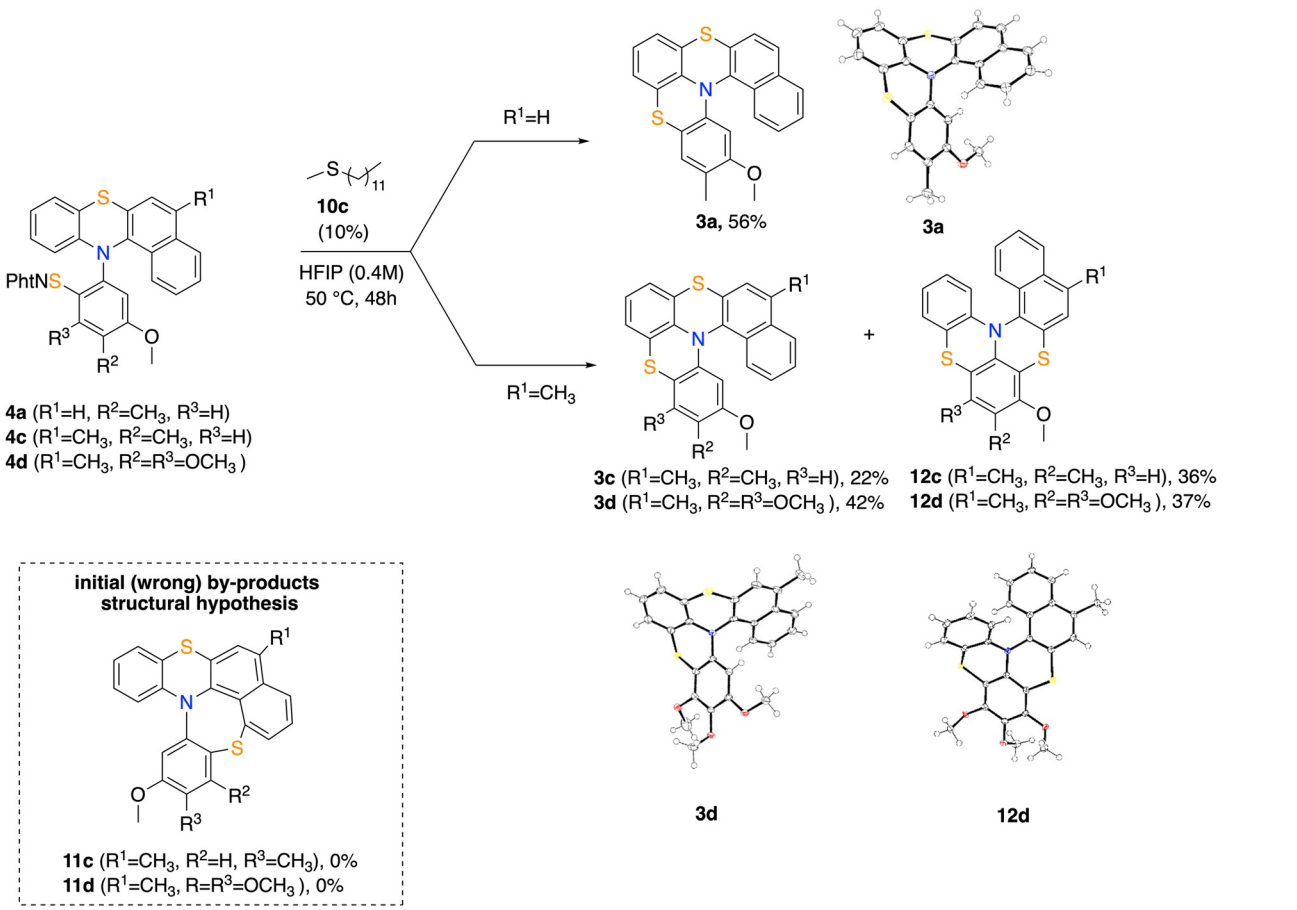


**Scheme 2** Cyclization reaction with the LB/HBD catalytic system. ORTEP diagrams of products **3a** (CCDC 2361198), **3d** (CCDC 2361200) and **12d** (CCDC 2361199) are shown. Other details are reported in the ESI.†

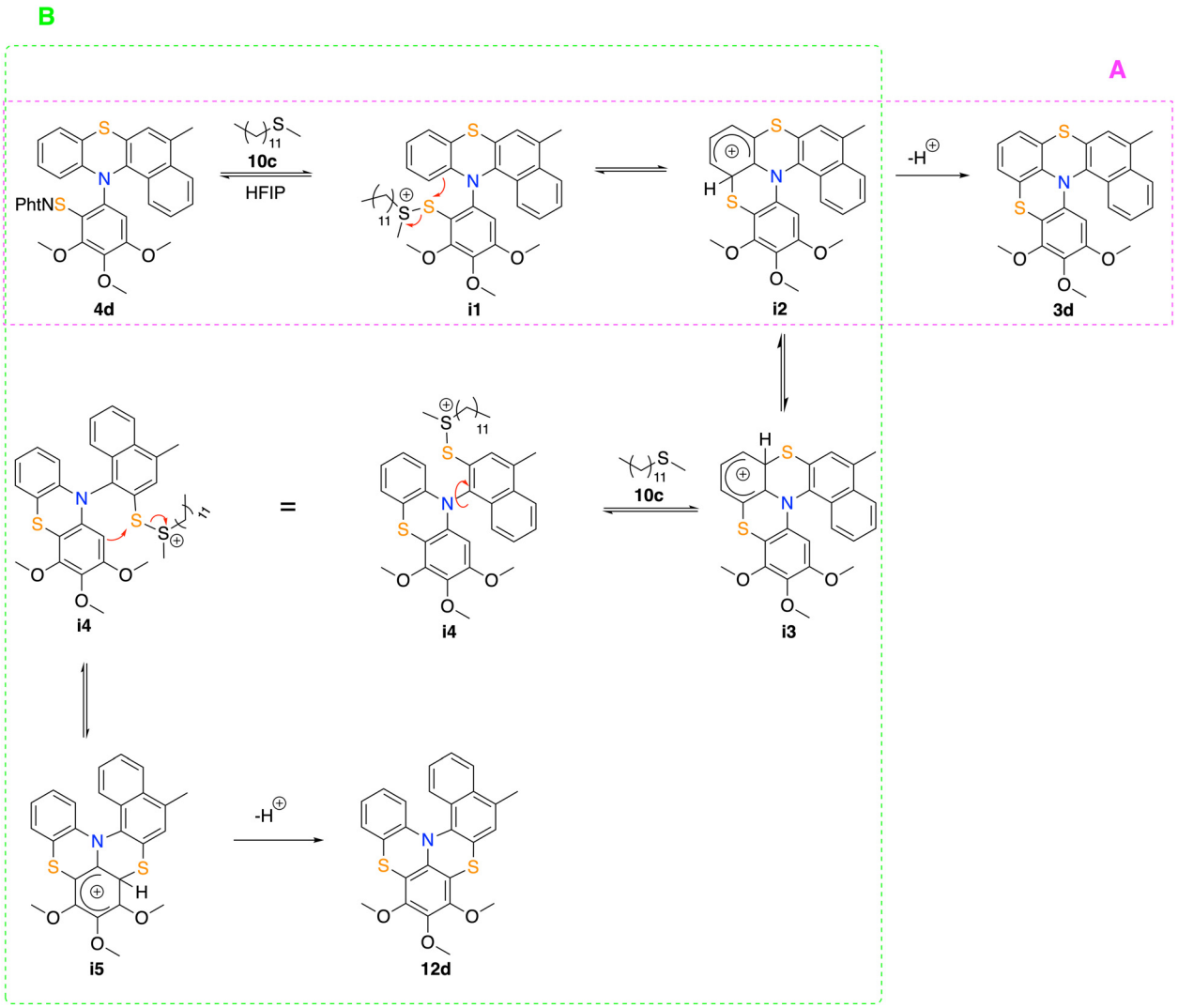


**Scheme 3** A possible rational mechanism for 3 *vs.* 12 thiabridged [5]helicene formation.

mation of the corresponding transposed helicene was observed, indicating that, reasonably, the **i2** → **3d** and **i5** → **12d** steps are not reversible. Surprisingly, when **10c** was replaced with **10b** for the cyclization of **4c** under the same reaction conditions as shown in Scheme 2, helicene **3c** was obtained as the major product with a $^{1}$H NMR yield of 51%, while the formation of the rearranged product was observed in trace amounts (*ca.* 5% $^{1}$H NMR yield), indicating that the regioselectivity of the reaction can be efficiently tuned by simply changing the Lewis base catalyst.

## Optical resolution

Having optimized the chemical resolution of derivatives **1**,[33] we envisaged that the presence of an additional aryl ring in the helical backbone could be beneficial for the resolution efficiency of compounds **3** and **12** due to steric interactions, therefore avoiding the troublesome insertion of the chiral auxiliary *ortho* to the nitrogen atom. Therefore, derivative **3a** was demethylated with $BBr_3$ to give phenol (***rac*)-3HelOH** (*i.e.* with the –OH function *meta* to the nitrogen). (***rac*)-3HelOH** was esterified with (*1S*)-(−)-camphanic acid (**13**), under the previously optimized reaction conditions,[33] to give a mixture of diastereomeric esters **3D1** and **3D2** that showed a slightly different behavior on TLC with a $\Delta R_f$ value of roughly 0.04. Indeed, the two esters were successfully isolated by flash chromatography on silica gel using $CH_2Cl_2$ : petroleum ether–2 : 1 as an eluent to give **3D1** (38% yield, $R_f$ = 0.55) and **3D2** (37% yield, $R_f$ = 0.51). Optical rotation was measured and gave $[\alpha]_D^{25}$ = +143 ($c$ = 0.2, $CH_2Cl_2$) for **3D1** and $[\alpha]_D^{25}$ = −146 ($c$ = 0.2, $CH_2Cl_2$) for **3D2**. Basic hydrolysis of the diastereomeric esters provided helicenes (+)-**3HelOH** and (−)-**3HelOH**, respectively, in a quantitative yield. HPLC analysis with a chiral stationary phase showed that (+)-**3HelOH** $[\alpha]_D^{25}$ +104 ($c$ = 0.2, $CH_2Cl_2$) exhibits an enantiomeric ratio of 1 : 99 (ee = 98%), while (−)-**3HelOH** $[\alpha]_D^{25}$ = −102 ($c$ = 0.2, $CH_2Cl_2$) exhibits an enantiomeric ratio of 97 : 3 (ee = 94%). These results demonstrate that

increasing the size of the *helical bay* by structural homologation, optical resolution can be achieved also for derivatives bearing the anchoring group not adjacent to the nitrogen. Interestingly, the $^1$H NMR spectra of **3D1** (see Fig. 2, inset, top) and **3D2** (see Fig. 2, inset, bottom) appear very similar, being two of the three methyl groups of the camphanic moiety, the sole functional groups that resonate (slightly) differently.

### Semipreparative CSP-HPLC resolution

Derivatives **3c** and **12d** were successfully resolved by semipreparative HPLC using CHIRALPAK IG as a chiral stationary phase. Optical rotation of the resolved **12d** was measured and gave $[\alpha]_D^{25}$ = –81 ($c$ = 0.07, $CH_2Cl_2$) for (–)-**12d** (first eluted, ee > 99%) and $[\alpha]_D^{25}$ = +76 ($c$ = 0.07, $CH_2Cl_2$) for (+)-**12d** (second eluted, ee = 94%), while for **3c** it gave $[\alpha]_D^{26}$ = +213 ($c$ = 0.03, $CH_2Cl_2$) for (+)-**3c** (first eluted, ee > 99%) and $[\alpha]_D^{26}$ = –213 ($c$ = 0.03, $CH_2Cl_2$) for (–)-**3c** (second eluted, ee > 99%). Regrettably, for derivatives **3d** and **12c**, the semipreparative resolution using CHIRALPAK IG as the chiral stationary phase was unsuccessful. Other CSPs are under investigation.

### Configurational stability of the thiabridged [5]helicenes

With the enantiopure compounds **3c** and **12d** in hand, we focused on the evaluation of their configurational stability. Enantiopure (+)-**12d** (ee > 99%) was dissolved in *n*-decane (1 mg mL$^{-1}$) and heated at increasing temperatures, 60 °C, 80 °C, 100 °C, 120 °C, 140 °C and at reflux (174 °C) for 2 hours. The solutions were cooled at rt and CSP-HPLC analysis was carried out. To our great satisfaction, no racemization was observed, even after 2 h at reflux, indicating that thiabridged [5]helicenes are significantly more stable than the corresponding thiabridged [4]helicenes, which showed a significant racemization rate at 121 °C in *n*-decane.[25] This allowed it to be estimated (see ESI†) that the racemization energy barrier for these [5]helicenes is higher than 40 kcal mol$^{-1}$.

### Chiroptical properties

The chiroptical properties of [5]helicenes **3HelOH**, **3c** and **12d**, namely ECD (electronic circular dichroism) and CPL (circularly polarized luminescence), have been investigated also with the aim to assign the absolute configuration by means of TD-DFT calculations. All spectra have been recorded in dichloromethane solutions. The ECD spectra (Fig. 3) are quite similar for the three compounds: a long wavelength broad CD band at *ca.* 395 nm; a band at *ca.* 325 nm and a band at 250 nm, both of the opposite sign to the first feature at 395 nm. In these three cases, the longest wavelength/lowest energy band presents a dissymmetry ratio $g_{abs} = \Delta A/A$ of about 0.8–0.9 × 10$^{-2}$, comparable to that of the second feature and higher than the one associated with the shorter wavelength region. Comparing the experimental and calculated ECD spectra, one can associ-

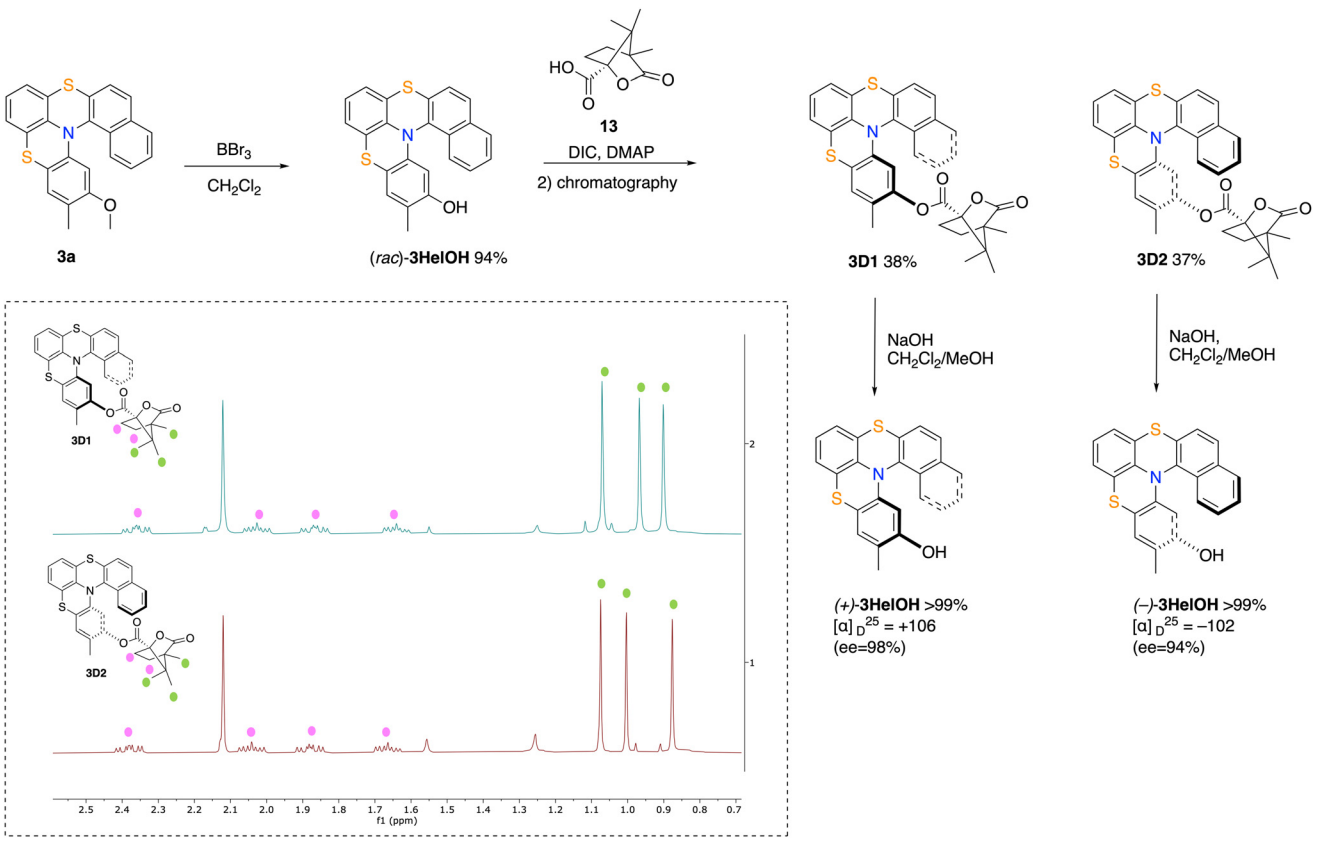


Fig. 2 Optical resolution of helicene **3a** using (1*S*)-camphanic acid as a chiral auxiliary. Inset: $^1$H NMR spectra of **3D1** (top) and **3D2** (bottom).

 

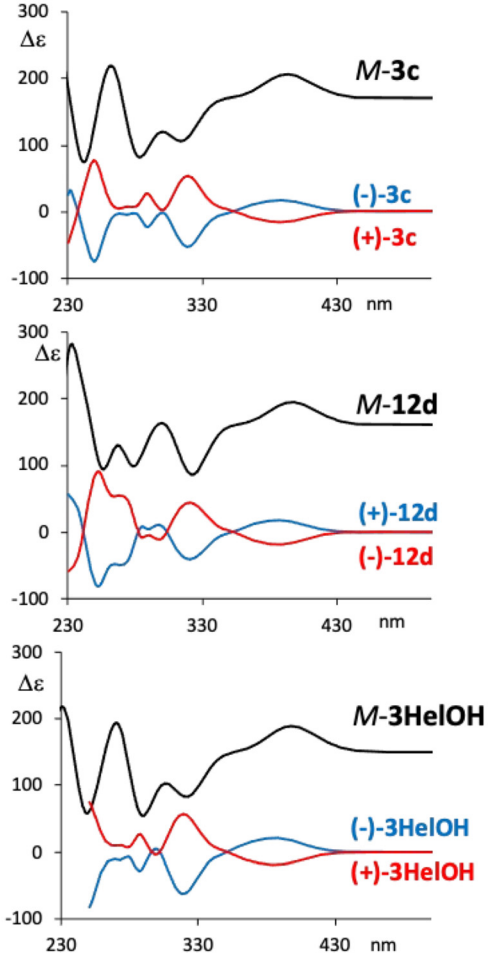


**Fig. 3** Experimental (red and blue lines for the two enantiomers) and calculated ECD spectra for the *M* (black lines) configuration of **3HelOH**, **3c** and **12d**. Calculations were performed at the TD-DFT/M06/cc-pVTZ/PCM(DCM) level of theory.

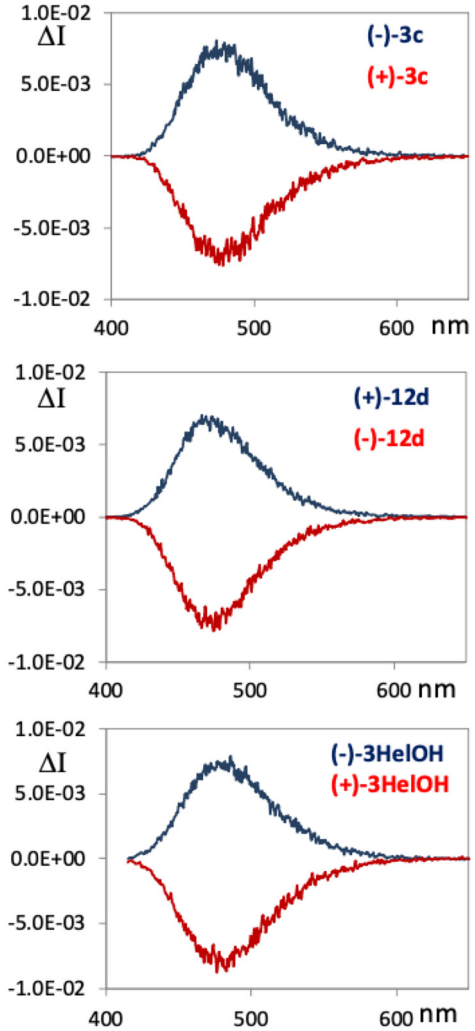


**Fig. 4** Experimental CPL spectra for the two enantiomers of **3HelOH**, **3c** and **12d**. CPL has been plotted after normalizing the fluorescence signal recorded with the same apparatus.

ate the positive first CD band (and the two other main negative bands) (Fig. 3, blue lines) to the *M* configuration (Fig. 3, black lines). In Fig. 4, we also report the experimental CPL spectra for the two eluted fractions of **3HelOH**, **3c** and **12d**. All three compounds behave very similarly, presenting a CPL band at about 480 nm. It is worth noting that the sign of the CPL bands correlates with the sign of the longest wavelength ECD band reported in Fig. 3. The dissymmetry ratio for CPL, $g_{lum} = \Delta I/I = 2(I_L - I_R) - (I_L + I_R)$, is about $0.8 \times 10^{-2}$ (similar to the $g_{abs}$ of the lowest energy transition) for all three compounds, which is a quite large value, since it is in the upper limit among simple organic compounds.[37,38]

We recall here that the spectra of simple carbo-helicenes present helical-sense responsive and substituent-sensitive chiroptical ECD features.[39] The latter, responsible also for CPL, are generally weak and dominated by vibronic contributions; on the contrary, the particular structure of the compounds under study here promotes the enhancement of the chiroptical properties: in fact the high dissymmetry ratio is in line with what is observed on an analogous thiabridged [6]helicene.[40] The present work confirms that substituents do not perturb this response and that the five-membered helicenes studied here exhibit chiroptical properties comparable to the longer one. We should add some comments about optical rotation (OR): as one may notice from Fig. 3, within this set of molecules it appears difficult to correlate the OR sign with the configuration. It was previously observed that shorter analogous helicenes, *i.e.* thiabridged [4]helicenes,[25,33] present a negative OR at 589 nm associated with the *M* configuration, while longer ones, in particular a thiabridged [6]helicene, present positive OR.[40] In the [5]helicenes under study, we recorded negative optical rotation for **3HelOH** and **3c** associated with the *M* configuration, and positive optical rotation for **12d**. As a further check, we recorded optical rotatory dispersion (ORD) for the same compounds in dichloromethane solutions (see Experimental section for details) at different wavelengths, until 436 nm. According to the Kronig–Kramers relation,[41]

ORD can be calculated from the whole CD spectrum, and this implies that often the optical rotation at the sodium D-line ends up with the same sign as the first CD band.[42] This is not the case for **3HelOH** and **3c**. However, it is interesting to note that, performing OR measurements at lower wavelengths, the OR sign of **3c** and **3HelOH** inverts and one records positive OR at 436 nm (+4163 and +3898, respectively), in accordance with the sign of the ECD band set at 395 nm and as expected while approaching the anomalous dispersion region. Analogously, a positive value is obtained at 436 nm also for the previously mentioned [4]helicene,[33] showing a negative value at 589 nm for the *M* configuration; that is to say, that in all examined cases approaching the first band, optical rotation takes the sign of the ECD band, which correlates with the helicene configuration. These observations suggest that a consistent set of ORD data, and not only a single OR value at the sodium D-line, is recommended to assign the absolute configuration.

# Conclusions

In conclusion, thiabridged [5]helicenes can be obtained by our previously developed LB/HBD catalytic route. The resolution of these systems either chemically, by formation of diastereoisomeric (1*S*)-camphanic esters, or through semipreparative CSP-HPLC was, overall, simpler than the corresponding thiabridged [4]helicenes. On the other hand, [5]helicenes showed an exceptional chemical and configurational stability; in fact, after 2 hours at 174 °C in *n*-decane, no trace of decomposition or racemization was detected allowing a racemization $\Delta G^{\neq}$ barrier higher than 40 kcal $mol^{-1}$ to be estimated. Furthermore, the CPL activity with high dissymmetry ratio, taken together with the configurational stability, makes these compounds useful candidates for applications in material science.

# Experimental part

### General information

$^{1}H$ and $^{13}C$ NMR spectra were recorded with a Varian Mercury Plus 400, and a Varian Inova 400, using $CDCl_3$ as a solvent. Residual $CHCl_3$ at $\delta$ = 7.26 ppm and the central line of $CDCl_3$ at $\delta$ = 77.16 ppm were used as the reference of the $^{1}H$-NMR spectra and $^{13}C$ NMR spectra, respectively. FT-IR spectra were recorded with a spectrum two FT-IR spectrometer. ESI-MS spectra were recorded with a JEOL MStation JMS700. Melting points were measured with Stuart SMP50 automatic melting point apparatus. Optical rotation measurements were performed on a JASCO DIP-370 polarimeter (JASCO, Easton, MD, USA) and the specific rotation of the compounds was reported. All the reactions were monitored by TLC on commercially available precoated plates (silica gel 60 F 254) and the products were visualized with acidic vanillin solution. Silica gel 60 (230–400 mesh) was used for column chromatography. Dry solvents were obtained by The PureSolv Micro Solvent Purification System. Chloroform was washed with water several times and stored over calcium chloride. Triethylamine was freshly distilled over KOH before use. Reagents were purchased from Signa Aldrich and used as received, unless otherwise specified. Phthalimidesulfenyl chloride was prepared from the corresponding disulfide as reported elsewhere.[43] Benzo[*a*]phenothiazine **7a** was prepared according to literature procedures.[35] The preparation and characterization of benzo[*a*]phenothiazines **7b**, *N*-aryl benzo[*a*]phenothiazines **9a–9d** and sulfenylated derivatives **4a–4d** are reported in the ESI.†

### Experimental chiroptical properties

ECD/UV measurements were conducted with a Jasco 815SE instrument with 2 mm quartz cuvettes in dichloromethane. Fluorescence spectra were recorded on a Jasco FP8600 instrument and CPL spectra were recorded on a home-built apparatus[44] with 10 accumulation scans using 2 mm fluorescence quartz cuvettes. ORD measurements were carried out with a JASCO P-2000 polarimeter using dichloromethane solutions at 0.07 g per 100 mL, 0.13 g per 100 mL and 0.02 g per 100 mL for **3c**, **12d** and **3HelOH**, respectively, at four different wavelengths, 589 nm (Na lamp), 578 nm, 546 nm, and 435 nm (Hg lamp), with 10 measurements at each wavelength.

### Calculations

The optimized geometry and ECD spectra have been calculated through DFT and TD-DFT methods performed with the Gaussian16 suite of programs.[45] The M06/cc-pVTZ level of theory, including bulk solvent effects by the conductor version of the polarizable continuum model (PCM), has been used.

### HPLC resolution

An analytical (250 × 4.6 mm) column packed with Chiralpak IA chiral stationary phase was purchased from Chiral Technologies Europe. A semipreparative (250 × 4.6 mm) column packed with Chiralpak IG chiral stationary phase was purchased from Chiral Technologies Europe. The HPLC resolution of the products was performed on a HPLC Waters Alliance 2695 equipped with a 200 μL loop injector and a spectrophotometer UV Waters PDA 2996. For CSP-HPLC semipreparative resolution of **3c** and **12d**, the mobile phase, delivered at a flow rate of 3.5 mL $min^{-1}$, was hexane/$CH_2Cl_2$ 80/20. For CSP-HPLC analytical resolution of [5]helicene **3c**, the mobile phase, delivered at a flow rate of 0.7 mL $min^{-1}$, was hexane/$CH_2Cl_2$ 90/10 while for **12d** the mobile phase, delivered at a flow rate of 1.0 mL $min^{-1}$, was hexane/$CH_2Cl_2$ 80/20.

### Syntheses

**Helicene 3a.** A screw-capped vial was charged with **4a** (220 mg, 0.4 mmol), HFIP (1 mL) and sulfide **10c** (9 mg, 0.04 mmol). The suspension was stirred vigorously at 50 °C for 48 h. After that time, the mixture was cooled at rt, diluted with $CH_2Cl_2$ (100 mL), and washed with a saturated solution of $NaHCO_3$ (50 mL × 3) and brine (50 mL). The organic layer was collected, dried over $Na_2SO_4$, filtered, and the volatiles were removed *via* rotary evaporation. The crude product was puri-

 

fied by flash chromatography on silica gel ($CH_2Cl_2$ : petroleum ether–1 : 3) to obtain **3a** as a light-yellow solid (90 mg, 56% yield).

m.p. 225–227 °C (dec.). IR (ATR neat) $\nu$ = 1556, 1491, 1431, 1384, 1165, 804, 775 $cm^{-1}$. Anal. calcd for $C_{24}H_{17}NOS_2$: C, 72.15; H, 4.29; N, 3.51; S, 16.05. Found: C, 72.34; H, 4.29; N, 3.71; S, 16.21. $^1H$ NMR (400 MHz, $CDCl_3$, $\delta$): 7.78 (dd, $J$ = 8.2, 1.2 Hz, 1H), 7.66 (d, $J$ = 8.5 Hz, 1H), 7.58 (bd, $J$ = 8.6 Hz, 1H), 7.39–7.26 (m, 3H), 7.15–6.98 (m, 2H), 6.11 (s, 1H), 3.35 (s, 3H), 2.17 (s, 3H), ppm. $^{13}C$ NMR (100 MHz, $CDCl_3$, $\delta$): 157.9, 145.0, 142.0, 135.2, 134.2, 129.3, 129.1, 128.4, 127.3, 126.9, 126.65, 126.60, 126.4, 125.9, 125.7, 125.5, 125.2, 125.0, 123.8, 123.1, 116.8, 102.8, 55.6, 15.8, ppm.

**Helicenes 3c and 12c.** A screw-capped vial was charged with **4c** (100 mg, 0.18 mmol), HFIP (450 mL) and sulfide **10c** (4 mg, 0.02 mmol). The suspension was stirred vigorously at 50 °C for 48 h. After that time, the mixture was cooled at rt, diluted with $CH_2Cl_2$ (100 mL), and washed with a saturated solution of $NaHCO_3$ (50 mL × 3) and brine (50 mL). The organic layer was collected, dried over $Na_2SO_4$, filtered, and the volatiles were removed *via* rotary evaporation. The crude product was purified by flash chromatography on silica gel (gradient from $CH_2Cl_2$/petroleum ether 1 : 4 to $CH_2Cl_2$ : peteroleum ether–1 : 2) to obtain **3c** (F1) as a light-yellow solid (16 mg, 22% yield) and **12c** (F2) as a light-yellow solid (26 mg, 36% yield).

**3c**: m.p. 252–254 °C. IR (ATR neat) $\nu$ = 1598, 1555, 1483, 1430, 1231, 1163 $cm^{-1}$. Anal. calcd for $C_{25}H_{19}NOS_2$: C, 72.61; H, 4.63; N, 3.39; S, 15.50. Found: 72.91; H, 4.68; N, 3.52; S, 15.71. $^1H$ NMR (400 MHz, $CDCl_3$, $\delta$): 7.91 (bd, $J$ = 8.4 Hz, 1H), 7.61 (bd, $J$ = 8.6 Hz, 1H), 7.42–7.38 (m, 1H), 7.29–7.25 (m, 1H), 7.16 (bs, 1H), 7.11 (dd, $J$ = 7.4, 1.6 Hz, 1H), 7.08 (bs, 1H), 7.04–6.96 (m, 2H), 6.07 (s, 1H), 3.33 (s, 3H), 2.67 (s, 3H), 2.14 (s, 3H), ppm. $^{13}C$ NMR (100 MHz, $CDCl_3$, $\delta$): 157.9, 145.3, 142.1, 133.3, 133.2, 132.9, 129.3, 129.2, 127.1, 126.9, 126.6, 126.3, 126.0, 125.9, 125.2, 125.0, 124.9, 124.7, 124.3, 122.9, 116.6, 102.7, 55.7, 19.3, 15.8, ppm.

**12c**: m.p. 270 °C (dec.). IR (ATR neat) $\nu$ = 1595, 1557, 1486, 1461, 1437, 1356, 1220, 1177, 1160, 1052 $cm^{-1}$. Anal. calcd for $C_{25}H_{19}NOS_2$: C, 72.61; H, 4.63; N, 3.39; S, 15.50. Found: 72.82; H, 4.58; N, 3.57; S, 15.38. $^1H$ NMR (400 MHz, $CDCl_3$, $\delta$): 9.28 (bd, $J$ = 8.5 Hz, 1H), 8.44 (bd, $J$ = 8.2 Hz, 1H), 7.87 (bd, $J$ = 8.4 Hz, 1H), 7.62 (s, 1H), 7.40–6.08 (m, 6H), 6.97 (s, 1H), 3.70 (s, 3H), 2.65 (s, 3H), 1.89 (s, 3H), ppm. $^{13}C$ NMR (50 MHz, $CDCl_3$, $\delta$): 157.7, 150.0, 147.1, 140.2, 134.5, 132.9, 132.7, 132.0, 131.0, 128.9, 127.9, 127.4, 127.0, 126.8, 126.7, 125.7, 125.7, 125.4, 124.9, 124.3, 112.3, 55.4, 19.3, 15.6, ppm.

**Helicenes 3d and 12d.** A screw-capped vial was charged with **4d** (100 mg, 0.17 mmol), HFIP (450 mL) and sulfide **10c** (4 mg, 0.02 mmol). The suspension was stirred vigorously at 50 °C for 48 h. After that time, the mixture was cooled at rt, diluted with $CH_2Cl_2$ (100 mL), and washed with a saturated solution of $NaHCO_3$ (50 mL × 3) and brine (50 mL). The organic layer was collected, dried over $Na_2SO_4$, filtered, and the volatiles were removed *via* rotary evaporation. The crude product was purified by flash chromatography on silica gel ($CH_2Cl_2$ : petroleum ether–7 : 3) to obtain **12d** (F1) as a light-yellow solid (28 mg, 37% yield) and **3d** (F2) as a light-yellow solid (32 mg, 42% yield).

**3d**: m.p. 222–223 °C. IR (ATR neat) $\nu$ = 1592, 1575, 1456, 1444, 1403, 1386, 1087, 1021 $cm^{-1}$. Anal. calcd for $C_{26}H_{21}NO_3S_2$: C, 67.95; H, 4.61; N, 3.05; S, 13.95. Found: C, 67.86; H, 4.92; N, 2.88; S, 13.86. $^1H$ NMR (400 MHz, $CDCl_3$, $\delta$): 7.90 (bd, $J$ = 8.4 Hz, 1H), 7.59 (bd, $J$ = 8.6 Hz, 1H), 7.42–7.38 (m, 1H), 7.30–7.26 (m, 1H), 7.16–7.14 (m, 2H), 7.04–6.96 (m, 2H), 5.93 (s, 1H), 4.03 (s, 3H), 3.83 (s, 3H), 3.36 (s, 3H), 2.66 (s, 3H), ppm. $^{13}C$ NMR (100 MHz, $CDCl_3$, $\delta$): 153.4, 150.1, 142.3, 142.0, 139.0, 133.2, 133.1, 133.0, 128.4, 127.1, 126.9, 126.5, 126.4, 126.1, 126.0, 125.6, 125.3, 124.9, 124.7, 124.1, 112.1, 100.0, 61.4 (2C), 56.3, 19.3, ppm.

**12d**: m.p. 204–207 °C. IR (ATR solid) $\nu$ = 1580, 1557, 1479, 1434, 1422, 1385, 1242, 1106, 1016 $cm^{-1}$. Anal. calcd for $C_{26}H_{21}NO_3S_2$: C, 67.95; H, 4.61; N, 3.05; S, 13.95. Found: C, 67.66; H, 4.82; N, 2.98; S, 13.55. $^1H$ NMR (400 MHz, $CDCl_3$, $\delta$): 7.91 (bd, $J$ = 8.4 Hz, 1H), 7.52 (bd, $J$ = 8.6 Hz, 1H), 7.41–7.37 (m, 2H), 7.26–7.22 (m, 1H), 7.19 (bs, 1H), 6.99 (td, $J$ = 7.5, 1.4 Hz, 1H), 6.93 (td, $J$ = 7.6, 1.6 Hz, 1H), 6.52 (dd, $J$ = 7.9, 1.4 Hz, 1H), 3.95 (s, 3H), 3.92 (s, 3H), 3.87 (s, 3H), 2.67 (s, 3H), ppm. $^{13}C$ NMR (100 MHz, $CDCl_3$, $\delta$): 148.9, 148.5, 146.7, 144.0, 137.4, 133.3, 132.9, 132.6, 128.2, 127.6, 127.0, 126.8, 126.34, 126.32, 126.1, 125.6, 124.8, 124.1, 123.7, 119.1, 118.2, 115.9, 61.5, 61.4, 61.3, 19.3, ppm.

**Phenol (*rac*)-3HelOH.** To a solution of helicene **3a** (55 mg, 0.14 mmol) in 1.4 mL of $CH_2Cl_2$, a 1 M solution of $BBr_3$ in $CH_2Cl_2$ (410 µL, 3.0 equiv.) was added at 0 °C *via* a syringe. The ice bath was removed after 10 min and the mixture was stirred at rt for 5 h. After that time, the mixture was poured into ice and diluted with AcOEt (20 mL), washed with a saturated solution of $NaHCO_3$ (8 mL × 3) and water (8 mL). The organic layers were collected, dried over $Na_2SO_4$, filtered and the volatiles were removed *via* rotary evaporation. The crude material was purified by flash chromatography on silica gel (petroleum ether : $CH_2Cl_2$–2 : 3) to afford **(*rac*)-3HelOH** as a white solid (53 mg, quantitative yield). m.p. 255 °C (dec.). IR (ATR neat) $\nu$ = 3542, 1431 $cm^{-1}$ Anal. calcd for $C_{23}H_{15}NOS_2$: C, 71.66;%; H 3.92%; N 3.63%; found: C, 71.22;%; H 3.57%; N 3.77%.$^1H$ NMR (400 MHz, $CDCl_3$, $\delta$): 7.76 (d, 1H, $J$ = 8.1 Hz), 7.64 (d, 1H, $J$ = 8.7 Hz), 7.57 (d, 1H, $J$ = 8.6 Hz), 7.38–7.34 (m, 1H), 7.30–7.27 (m, 2H), 7.12 (dd, 1H, $J$ = 7.2, 1.8 Hz), 7.08 (bs, 1H), 7.04–6.97 (m, 2H), 6.06 (s, 1H), 4.44 (s, 1H), 2.16 (s, 3H), ppm. $^{13}C$ NMR (100 MHz, $CDCl_3$, $\delta$): 153.8, 145.3, 141.8, 134.9, 134.3, 129.8, 129.1, 128.5, 127.5, 127.0, 126.8, 126.6, 126.4, 126.0, 125.8, 125.5, 125.2, 125.1, 123.8, 120.4, 117.5, 106.8, 15.4, ppm.

**Camphanates 3D1 and 3D2.** The general procedure from **(*rac*)-3HelOH** (42 mg, 0.11 mmol) and (1*S*)-(−)-camphanic acid (**13**) (32 mg, 0.16 mmol) was followed, kept for 12 h at room temperature. The crude product was purified by flash chromatography on silica gel (petroleum ether/$CH_2Cl_2$ 1/2, **3D1** $R_f$ = 0.55, **3D2** $R_f$ = 0.51) to afford product **3D1** (24 mg, 38% yield) as a white solid and product **3D2** (23 mg, 37% yield) as a white solid.

**3D1**: IR (ATR neat) $\nu$ = 1791, 1435 $cm^{-1}$ Anal. calcd for $C_{33}H_{27}NO_4S_2$: C, 70.07%; H 4.81%; N 2.48%; found: C, 70.49; %; H 5.14%; N 2.77%. $^1H$ NMR (400 MHz, $CDCl_3$, $\delta$): 7.76 (d, 1H, $J$ = 8.1 Hz), 7.65 (d, 1H, $J$ = 8.6 Hz), 7.48 (d, 1H, $J$ = 8.6 Hz) 7.39–7.35 (m, 1 H), 7.30–7.22 (m, 3H), 7.11 (dd, 1H, $J$ = 7.2, 1.9 Hz), 7.05–6.98 (m, 2H), 6.23 (s, 1H), 2.40–2.33 (m, 1H), 2.12 (s, 3H), 2.06–1.99 (m, 1H), 1.90–1.83 (m, 1H), 1.67–1.61 (m, 1H), 1.07 (s, 3H), 0.97 (s, 3H) 0.90 (s, 3H), ppm. $^{13}C$ NMR (100 MHz, $CDCl_3$, $\delta$): 177.8, 165.6, 148.5, 145.1, 141.4, 134.4, 134.3, 129.9, 128.6, 128.1, 127.6, 127.0, 126.84, 126.77, 126.7, 126.02, 125.97, 125.9, 125.5, 125.41, 125.39, 125.0, 123.5, 112.8, 90.8, 54.9, 54.6, 31.2, 29.0, 16.9, 16.8, 16.3, 9.8, ppm. Opt. Rot.: $[\alpha]_D^{20}$ +143 ($c$ = 0.2 in $CH_2Cl_2$) (99 : 1 dr).

**3D2**: IR (ATR neat) $\nu$ = 1791, 1435, $cm^{-1}$. Anal. calcd for $C_{33}H_{27}NO_4S_2$: C, 70.07%; H 4.81%; N 2.48%; found: C, 70.37%; H 4.74%; N 2.78%. $^1H$ NMR (400 MHz, $CDCl_3$, $\delta$): 7.77 (d, 1H, $J$ = 8.1 Hz), 7.66 (d, 1H, $J$ = 8.5 Hz), 7.50 (d, 1H, $J$ = 8.5 Hz) 7.40–7.35 (m, 1 H), 7.31–7.23 (m, 3H), 7.12 (dd, 1H, $J$ = 6.9, 2.1 Hz), 7.07–7.00 (m, 2H), 6.22 (s, 1H), 2.42–2.35 (m, 1H), 2.12 (s, 3H), 2.08–2.01 (m, 1H), 1.92–1.84 (m, 1H), 1.70–1.63 (m, 1H), 1.07 (s, 3H), 1.00 (s, 3H) 0.88 (s, 3H), ppm. $^{13}C$ NMR (100 MHz, $CDCl_3$, $\delta$): 177.8, 165.5, 148.5, 145.1, 141.4, 134.4, 134.3, 129.9, 128.5, 128.1, 127.6, 127.0, 126.9, 126.8, 126.7, 126.00, 125.97, 125.9, 125.5, 125.44, 125.39, 125.1, 123.5, 112.8, 90.8, 54.9, 54.4, 31.1, 29.0, 16.90, 16.87, 16.2, 9.8, ppm. Opt. Rot.: $[\alpha]_D^{20}$ −146 ($c$ = 0.2 in $CH_2Cl_2$) (97 : 3 dr).

## Data availability

The data that support the findings of this study, including $^1H$ and $^{13}C$ NMR spectra, CSP-HPLC traces of all the resolved compounds, and details of the racemization energy estimation, are available in the ESI of this article. Crystallographic data for **3a**, **3d**, and **12d** has been deposited at the Cambridge Crystallographic Data Centre under 2361198 (**3a**) 2361200 (**3d**) and 2361199 (**12d**) and can be obtained from **https://www.ccdc.cam.ac.uk/structures/**.†

## Conflicts of interest

There are no conflicts to declare.

## Acknowledgements

Support provided by the MUR – Progetto Dipartimenti di Eccellenza 2023–2027 (DICUS 2.0) to the Department of Chemistry "Ugo Schiff" of the University of Florence and by the Horizon Europe Program through the ERC-Synergy project CASTLE (proj. no. 101071533) is acknowledged. The authors thank Dr Cristina Faggi for X-ray analyses. The Big & Open Data Innovation Laboratory (BODaILab) of the University of Brescia and Computing Center CINECA (Bologna, Italy) are acknowledged for providing high-performance computing facilities.

## References

1 K. Yavari, P. Aillard, Y. Zhang, F. Nuter, P. Retailleau, A. Voituriez and A. Marinetti, *Angew Chem., Int. Ed.*, 2014, **53**, 861–865.
2 N. Takenaka, J. Chen, B. Captain, R. S. Sarangthem and A. Chandrakumar, *J. Am. Chem. Soc.*, 2010, **132**, 4536–4537.
3 D. Sakamoto, I. G. Sánchez, J. Rybáček, J. Vacek, L. Bednárová, M. Pazderková, R. Pohl, I. Císařová, I. G. Stará and I. Starý, *ACS Catal.*, 2022, **12**, 10793–10800.
4 B. Lousen, S. K. Pedersen, D. M. Răsădean, G. D. Pantoș and M. Pittelkow, *Chem. – Eur. J.*, 2021, **27**, 6064–6069.
5 P. A. Summers, A. P. Thomas, T. Kench, J. B. Vannier, M. K. Kuimova and R. Vilar, *Chem. Sci.*, 2021, **12**, 14624–14634.
6 J. L. Rushworth, A. R. Thawani, E. Fajardo-Ruiz, J. C. M. Meiring, C. Heise, A. J. P. White, A. Akhmanova, J. R. Brandt, O. Thorn-Seshold and M. J. Fuchter, *JACS Au*, 2022, **2**, 2561–2570.
7 T. R. Schulte, J. J. Holstein and G. H. Clever, *Angew. Chem., Int. Ed.*, 2019, **58**, 5562–5566.
8 A. U. Malik, F. Gan, C. Shen, N. Yu, R. Wang, J. Crassous, M. Shu and H. Qiu, *J. Am. Chem. Soc.*, 2018, **140**, 2769–2772.
9 V. Kiran, S. P. Mathew, S. R. Cohen, I. Hernández Delgado, J. Lacour and R. Naaman, *Adv. Mater.*, 2016, **28**, 1957–1962.
10 R. Rodríguez, C. Naranjo, A. Kumar, P. Matozzo, T. K. Das, Q. Zhu, N. Vanthuyne, R. Gómez, R. Naaman, L. Sánchez and J. Crassous, *J. Am. Chem. Soc.*, 2022, **144**, 7709–7719.
11 Y. Yang, R. C. da Costa, M. J. Fuchter and A. J. Campbell, *Nat. Photonics*, 2013, **7**, 634–638.
12 J. R. Brandt, X. Wang, Y. Yang, A. J. Campbell and M. J. Fuchter, *J. Am. Chem. Soc.*, 2016, **138**, 9743–9746.
13 W. Fu, V. Pelliccioli, M. von Geyso, P. Redero, C. Böhmer, M. Simon, C. Golz and M. Alcarazo, *Adv. Mater.*, 2023, 2211279.
14 T. Hartung, R. Machleid, M. Simon, C. Golz and M. Alcarazo, *Angew. Chem., Int. Ed.*, 2020, **59**, 5660.
15 V. Pelliccioli, T. Hartung, M. Simon, C. Golz, E. Licandro, S. Cauteruccio and M. Alcarazo, *Angew. Chem., Int. Ed.*, 2022, **61**, e202114577.
16 L. D. M. Nicholls, M. Marx, T. Hartung, E. González-Fernández, C. Golz and M. Alcarazo, *ACS Catal.*, 2018, **8**, 6079–6085.
17 P. Redero, T. Hartung, J. Zhang, L. D. M. Nicholls, G. Zichen, M. Simon, C. Golz and M. Alcarazo, *Angew. Chem., Int. Ed.*, 2020, **59**, 23527–23531.
18 E. González-Fernández, L. D. M. Nicholls, L. D. Schaaf, C. Farès, C. W. Lehmann and M. Alcarazo, *J. Am. Chem. Soc.*, 2017, **139**, 1428–1431.
19 C. Li, Y.-B. Shao, X. Gao, Z. Ren, C. Guo, M. Li and X. Li, *Nat. Commun.*, 2023, **14**, 3380.
20 K. Li, S. Huang, T. Liu, S. Jia and H. Yan, *J. Am. Chem. Soc.*, 2022, **144**, 7374–7381.
21 L. Kötzner, M. J. Webber, A. Martínez, C. Defusco and B. List, *Angew. Chem., Int. Ed.*, 2014, **53**, 5202–5205.

 

22 W. Liu, T. Qin, W. Xie, J. Zhou, Z. Ye and X. Yang, *Angew. Chem., Int. Ed.*, 2023, **62**, e202303430.
23 S. Menichetti, S. Cecchi, P. Procacci, M. Innocenti, L. Becucci, L. Franco and C. Viglianisi, *Chem. Commun.*, 2015, **51**, 11452–11454.
24 R. Amorati, L. Valgimigli, A. Baschieri, Y. Guo, F. Mollica, S. Menichetti, M. Lupi and C. Viglianisi, *ChemPhysChem*, 2021, **22**, 1446–1454.
25 G. Lamanna, C. Faggi, F. Gasparrini, A. Ciogli, C. Villani, P. J. Stephens, F. J. Devlin and S. Menichetti, *Chem. – Eur. J.*, 2008, **14**, 5747–5750.
26 N. Giaconi, A. L. Sorrentino, L. Poggini, M. Lupi, V. Polewczyk, G. Vinai, P. Torelli, A. Magnani, R. Sessoli, S. Menichetti, L. Sorace, C. Viglianisi and M. Mannini, *Angew Chem., Int. Ed.*, 2021, **60**, 15276–15280.
27 (*a*) N. Giaconi, L. Poggini, M. Lupi, M. Briganti, A. Kumar, T. K. Das, A. L. Sorrentino, C. Viglianisi, S. Menichetti, R. Naaman, R. Sessoli and M. Mannini, *ACS Nano*, 2023, **17**, 15189–15198; (*b*) N. Giaconi, M. Lupi, T. K. Das, A. Kumar, L. Poggini, C. Viglianisi, L. Sorace, S. Menichetti, R. Naaman, R. Sessoli and M. Mannini, *J. Mater. Chem. C*, 2024, **12**, 10029–10035.
28 H. Ando, H. Takamura, I. Kadota and K. Tanaka, *Chem. Commun.*, 2024, **60**, 4765–4768.
29 M. Lupi, O. Salmi, C. Viglianisi and S. Menichetti, *Adv. Synth. Catal.*, 2023, **365**, 1705–1712.
30 K. Usui, K. Yamamoto, T. Shimizu, M. Okazumi, B. Mei, Y. Demizu, M. Kurihara and H. Suemune, *J. Org. Chem.*, 2015, **80**, 6502–6508.
31 (*a*) T. Tsujihara, D. Y. Zhou, T. Suzuki, S. Tamura and T. Kawano, *Org. Lett.*, 2017, **19**, 3311–3314; (*b*) T. Thongpanchang, K. Paruch, T. J. Katz, A. L. Rheingold, K. C. Lam and L. Liable-Sands, *J. Org. Chem.*, 2000, **65**, 1850–1856; (*c*) F. Torricelli, J. Bosson, C. Besnard, M. Chekini, T. Bürgi and J. Lacour, *Angew. Chem., Int. Ed.*, 2013, **52**, 1796–1800; (*d*) E. H. Bhalodi, K. N. Patel and A. V. Bedekar, *Tetrahedron*, 2022, **114**, 132761.
32 (*a*) C. Herse, D. Bas, F. C. Krebs, T. Bürgi, J. Weber, T. Wesolowski, B. W. Laursen and J. Lacour, *Angew. Chem., Int. Ed.*, 2003, **42**, 3162–3166; (*b*) B. Laleu, P. Mobian, C. Herse, B. W. Laursen, G. Hopfgartner, G. Bernardinelli and J. Lacour, *Angew. Chem., Int. Ed.*, 2005, **44**, 1879–1883.
33 M. Lupi, M. Onori, S. Menichetti, S. Abbate, G. Longhi and C. Viglianisi, *Molecules*, 2022, **27**, 1160.
34 G. R. Kiel, H. M. Bergman, A. E. Samkian, N. J. Schuster, R. C. Handford, A. J. Rothenberger, R. Gomez-Bombarelli, C. Nuckolls and T. Don Tilley, *J. Am. Chem. Soc.*, 2022, **144**, 23421–23427.
35 Y. Lin, G. Lu, R. Wang and W. Yi, *Org. Lett.*, 2016, **18**, 6424–6427.
36 All attempts to use methoxy-substituted tetralones as starting materials failed leading to oxidative degradation.
37 H. Tanaka, Y. Inoue and T. Mori, *ChemPhotoChem*, 2018, **2**, 386–402.
38 G. Mazzeo, S. Ghidinelli, R. Ruzziconi, M. Grandi, S. Abbate and G. Longhi, *ChemPhotoChem*, 2022, **6**, e202100222.
39 S. Abbate, G. Longhi, F. Lebon, E. Castiglioni, S. Superchi, L. Pisani, F. Fontana, F. Torricelli, T. Caronna, C. Villani, R. Sabia, M. Tommasini, A. Lucotti, D. Mendola, A. Mele and D. A. Lightner, *J. Phys. Chem. C*, 2014, **118**, 1682–1695.
40 G. Longhi, E. Castiglioni, C. Villani, R. Sabia, S. Menichetti, C. Viglianisi, F. Devlin and S. Abbate, *J. Photochem. Photobiol., A*, 2016, **331**, 138–145.
41 A. Moskowitz, *Optical Rotatory Dispersion*, ed. C. Djerassi, McGraw-Hill Book Co, New York, 1960, vol. 151.
42 E. Giorgio, R. G. Viglione, R. Zanasi and C. Rosini, *J. Am. Chem. Soc.*, 2004, **126**, 12968–12976.
43 C. Viglianisi, E. Marcantoni, V. Carapacchi, S. Menichetti and L. Marsili, *Eur. J. Org. Chem.*, 2014, 6405–6410.
44 E. Castiglioni, S. Abbate and G. Longhi, *Appl. Spectrosc.*, 2010, **64**, 1416–1419.
45 M. J. Frisch, G. W. Trucks, H. B. Schlegel, G. E. Scuseria, M. A. Robb, J. R. Cheeseman, G. Scalmani, V. Barone, G. A. Petersson, H. Nakatsuji, X. Li, M. Caricato, A. V. Marenich, J. Bloino, B. G. Janesko, R. Gomperts, B. Mennucci, H. P. Hratchian, J. V. Ortiz, A. F. Izmaylov, J. L. Sonnenberg, D. Williams, F. Ding, F. Lipparini, F. Egidi, J. Goings, B. Peng, A. Petrone, T. Henderson, D. Ranasinghe, V. G. Zakrzewski, J. Gao, N. Rega, G. Zheng, W. Liang, M. Hada, M. Ehara, K. Toyota, R. Fukuda, J. Hasegawa, M. Ishida, T. Nakajima, Y. Honda, O. Kitao, H. Nakai, T. Vreven, K. Throssell, J. A. Montgomery Jr., J. E. Peralta, F. Ogliaro, M. J. Bearpark, J. J. Heyd, E. N. Brothers, K. N. Kudin, V. N. Staroverov, T. A. Keith, R. Kobayashi, J. Normand, K. Raghavachari, A. P. Rendell, J. C. Burant, S. S. Iyengar, J. Tomasi, M. Cossi, J. M. Millam, M. Klene, C. Adamo, R. Cammi, J. W. Ochterski, R. L. Martin, K. Morokuma, O. Farkas, J. B. Foresman and D. J. Fox, *Gaussian 16, Rev. C.01*, 2016.